International Journal of Antimicrobial Agents 54 (2019) 592–600

Contents lists available at ScienceDirect

International Journal of Antimicrobial Agents

journal homepage: www.elsevier.com/locate/ijantimicag

Potential impact of the antirheumatic agent auranofin on proviral HIV-1 DNA in individuals under intensified antiretroviral therapy: Results from a randomised clinical trial

Ricardo Sobhie Diaz[a], Iart Luca Shytaj[b,c], Leila B. Giron[a,d], Benedikt Obermaier[b,c], Ermelindo della Libera Jr[a], Juliana Galinskas[a], Danilo Dias[a], James Hunter[a], Mario Janini[a], Gisele Gosuen[a], Paulo Abrão Ferreira[a], Maria Cecilia Sucupira[a], Juliana Maricato[a], Oliver Fackler[b,c], Marina Lusic[b,c], Andrea Savarino[e,*], SPARC Working Group

[a] Federal University of Sao Paulo, Infectious Diseases Department, São Paulo, 04021-001, Brazil
[b] Heidelberg University Hospital, Department of Infectious Diseases, Heidelberg 69120, Germany
[c] German Center for Infection Research, Heidelberg 69120, Germany
[d] The Wistar Institute, Philadelphia, PA, USA
[e] Department of Infectious Diseases, Istituto Superiore di Sanità, Viale Regina Elena 299, I-00161 Rome, Italy

ARTICLE INFO

Article history:
Received 23 April 2019
Accepted 1 August 2019

Editor: Philippe Colson

Keywords:
HIV cure
HIV reservoir
Disease-modifying antirheumatic agent
Proviral DNA
Viral evolution
Antiproliferative agent

ABSTRACT

Antiretroviral therapy (ART) is typically composed of a combination of three antiretroviral drugs and is the treatment of choice for people with human immunodeficiency virus type 1/acquired immune deficiency syndrome (HIV-1/AIDS). However, it is unable to impact on viral reservoirs, which harbour latent HIV-1 genomes that are able to reignite the infection upon treatment suspension. The aim of this study was to provide an estimate of the safety of the disease-modifying antirheumatic agent auranofin and its impact on the HIV-1 reservoir in humans under intensified ART. For this purpose, an interim analysis was conducted of three of the six arms of the NCT02961829 clinical trial (five patients each) with: no intervention, i.e. continuation of first-line ART; intensified ART (ART + dolutegravir and maraviroc); and intensified ART plus auranofin. Auranofin treatment was found to be well tolerated. No major adverse events were detected apart from a transient decrease in $CD4^+$ T-cell counts at Weeks 8 and 12. Auranofin decreased total viral DNA in peripheral blood mononuclear cells compared with ART-only regimens at Week 20 ($P = 0.036$) and induced a decrease in integrated viral DNA as quantified by Alu PCR. Despite the limited number of patient-derived sequences available in this study, phylogenetic analyses of *nef* sequences support the idea that auranofin may impact on the viral reservoir. [ClinicalTrials.gov ID: NCT02961829]

1. Introduction

Gold salts, which have been used for decades in the treatment of rheumatoid arthritis, possess effects that render them promising candidates for antimicrobial therapy [1–3]. The anti-infective effects of gold salts were first hypothesised during the Italian Renaissance and were then demonstrated by Robert Koch in 1890 [4]. Despite almost a century of stagnation, the use of gold salts as antimicrobial agents has experienced a revival in the 21st century and they are being explored as promising therapeutic agents against bacterial [1,2], parasitic [3], fungal [5] and viral [6] diseases. Moreover, the anti-lymphoproliferative effect of gold salts, which have long been employed for the treatment of rheumatoid arthritis, may provide a therapeutic benefit in viral diseases, particularly those that are complicated by virus-related inflammation [6]. Among these, one promising application resides in the search for a cure for human immunodeficiency virus type 1 (HIV-1) infection, wherein gold salts may become a novel class of agents acting by a mechanism different from that of current antiretroviral therapies (ARTs).

HIV-1 infection cannot be eradicated by ART. Latently infected cells, mainly memory $CD4^+$ T-cells that harbour the virus in a dormant state and cannot be targeted by either ART or the immune system, persist during therapy and proliferate both by homeostatic and antigen-driven proliferation [7–9]. This concept has been confirmed by phylogenetic analysis of sequenced proviral DNA during

* Corresponding author. Tel.: +39 06 4990 2305; fax: +39 06 4990 3561.
E-mail address: andrea.savarino@iss.it (A. Savarino).

https://doi.org/10.1016/j.ijantimicag.2019.08.001

ART. The same technique has also suggested that maintenance of the viral reservoir in vivo is mainly due to a limited number of proliferating HIV-1-infected cells [10]. Several attempts to target the HIV-1 reservoir have been tested in clinical trials. These include the 'shock and kill' approach (reversing HIV-1 latency to render the infected cells targetable), therapeutic vaccines, gene therapy, and broad-spectrum combinations of monoclonal antibodies [8,11]. At present, however, HIV-1 has only been eradicated in two individuals who were subjected to myeloablative chemotherapy and whose immune systems were replaced with those of donors resistant to R5 HIV-1 strains [12,13]. Therefore, an HIV-1 cure remains an unmet medical need. More so, since it was calculated that eliminating HIV-1 from the body only with current ART regimens would take an average time of approximately 70 years, a therapeutic timeframe that renders HIV-1 eradication unrealistic in a lifetime [8].

In the context of research for a cure for HIV-1, the gold salt auranofin was previously shown to have therapeutic potential in a macaque model of acquired immune deficiency syndrome (AIDS). Auranofin was able to induce a decay of viral DNA in peripheral blood of macaques infected with the HIV-1 homologue simian immunodeficiency virus SIVmac251 when used in combination with intensified ART [14]. This observation is in line with the antiproliferative effect of gold salts, which is exerted through inhibition of interleukin-2 (IL-2)-mediated signalling [15,16]. Moreover, other mechanisms may contribute to the impact exerted by auranofin on the viral reservoir, e.g. auranofin induces lymphocyte differentiation, especially in the memory compartment encompassing the viral reservoir [17], thus limiting its proliferative potential further.

A clinical trial (SPARC-7) recently conducted at the Federal University of Sao Paulo (Sao Paulo, Brazil) added to standard ART a number of experimental interventions [18] (ClinicalTrials.gov ID: NCT02961829; http://www.clinicaltrials.gov), including auranofin. Specifically, in this open-label randomised trial, 30 individuals on ART were randomised to six treatments lasting 48 weeks, as detailed in the Methods section. As auranofin has been hypothesised to be a potential candidate in a number of combination therapies aimed at an HIV-1 cure, other than that tested in the SPARC-7 trial [19], we decided to conduct an interim analysis to investigate the impact of this drug on the viral DNA dynamics using samples derived from SPARC-7.

Thus, the present study aimed to provide an estimate of the impact of auranofin on the HIV-1 reservoir in humans and to detail the effects of the first use of a gold compound with ART in a clinical setting.

2. Methods

2.1. Subjects and setting

Thirty individuals with viral loads suppressed by ART were enrolled in the SPARC-7 trial. Inclusion criteria were: males aged >18 years with documented HIV-1 infection; on ART for ≥2 years, without changes in the 24 weeks immediately prior to screening; HIV viral load <50 copies/mL and never >50 copies/mL on two consecutive occasions in the last 2 years; CD4 nadir >350 cells/μL; current CD4 count >500 cells/μL; and R5 HIV-1 infection at screening as defined by proviral DNA genotropism. Exclusion criteria were: any evidence of an active AIDS-defining condition; any significant acute medical illness in the past 8 weeks; pregnancy or breastfeeding owing to the possible teratogenicity of auranofin [20]; use in the 90 days prior to enrolment of systemic cytotoxic chemotherapy, investigational agents, immunomodulators, coumadin, warfarin or other coumadin-derivative anticoagulants; use of an agent definitely or possibly associated with an effect on the QT interval; receipt of compounds with histone deacetylase inhibitor-like activity, such as valproic acid or nicotinamide, within the last 30 days; known hypersensitivity to the components of gold salt, nicotinamide or its analogues; hepatitis B (HBsAg+) or hepatitis C (HCV-RNA+) virus infection; known renal insufficiency defined as a calculated creatinine clearance (Cockcroft–Gault formula) <60 mL/min; presence of a laboratory abnormality grade 3 or 4 with the exceptions of pancreatic amylase, cholesterol, triglyceride, gamma-glutamyl transferase and bilirubin; and presence of conditions that, in the investigators' opinion, could compromise safety or adherence to the trial protocol. The protocol was approved by the Human Subjects Review Committee of the Federal University of Sao Paulo.

Enrolled individuals were randomised to six groups: group 1, continuation of ART; group 2, intensified ART (ART + dolutegravir + maraviroc); group 3, intensified ART and nicotinamide (1000 mg once daily); group 4, intensified ART and auranofin (oral, 3 mg twice daily); group 5, partially intensified ART (dolutegravir) + dendritic cell vaccine; and group 6, partially intensified ART + nicotinamide + auranofin + dendritic cell vaccine (ClinicalTrials.gov ID: NCT02961829; Supplementary Fig. S1). Auranofin was used for the first 24 weeks. Antiretroviral drugs were administered at dosages in line with standard clinical guidelines. The allocation ratio was 1:1:1:1:1:1 and the interventions were conducted in parallel.

As this trial recruited participants for a long period, an interim analysis was conducted on the impact of auranofin on the viral reservoir due to the reasons detailed in the Introduction section. The potential in vivo effects of auranofin in peripheral blood mononuclear cell (PBMC) samples from groups 1, 2 and 4 were explored (Supplementary Fig. S1; Table 1). Groups 3 and 6 of this clinical trial were aimed at evaluating interventions unrelated to the anti-reservoir effect of auranofin and have therefore not been considered in the present study. The overall architecture and general conclusions of the entire clinical trial will be the object of a separate report. The primary outcome measure of the present interim analysis was the measurement of viral reservoir markers at 5 months of treatment, i.e. the time point at which the effects of auranofin are maximal [21].

2.2. Quantification of viral load

Viral load in plasma was quantified every 4 weeks using an Abbott RealTime HIV-1 Viral Load Assay (Abbott Laboratories, Lake Forest, IL, USA) running on an automated RNA extraction and detection platform m2000 (Abbott Laboratories) according to the manufacturer's instructions. The detection limit of the assay is 40 copies/mL.

2.3. Quantification of HIV-1 DNA

DNA from PBMCs was isolated using an AllPrep DNA/RNA Kit (QIAGEN, Ventura, CA, USA) as specified by the manufacturer and was quantified using a NanoDrop™ ND-1000 spectrophotometer (Thermo Fisher Scientific, Waltham, MA, USA). Total viral DNA was measured following a previously published procedure [22] after in-house analyses aimed at ruling out the effect of PCR inhibitors and secure maximal detection of viral DNA copies. Total HIV-1 DNA was measured by quantitative PCR (qPCR) using the HIV-1 LTR region as the target and the human CCR5 gene as the normaliser. Copy numbers were extrapolated from standard curves generated with plasmids harbouring two copies of the CCR5 gene and the HIV-1 LTR sequence. Briefly, the reaction mixture consisted of 1 × final concentration of 2 × Gene Expression Master Mix (Life Technologies, Carlsbad, CA, USA), 0.75 μM of each oligonucleotide, 0.3 μM of probe, 5 μL of sample diluted 1:10 or 1:20 depending on the

Table 1
Demographic, immunological and virological characteristics and treatment details of the individuals enrolled.

Group	CD4$^+$ T-cell nadir[a]	Sex	Age (years)	Viral load[b]	Baseline ART	Time of treatment initiation[c]
1	395	Male	29	78 753	TDF + 3TC + EFV	2013
1	534	Male	49	17 188	TDF + 3TC + FPV/r	2002
1	580	Male	34	110 000	TDF + FTC + NVP	2004
1	658	Male	53	52 312	TDF + 3TC + EFV	2013
1	758	Male	33	9736	TDF + FTC + RAL	2014
2	492	Male	28	11 762	TDF + 3TC + EFV	2013
2	566	Male	60	97 000	AZT + 3TC + NVP	2007
2	604	Male	39	7512	AZT + 3TC+ATV/r	2013
2	661	Male	35	55 000	TDF + 3TC + EFV	2012
2	683	Male	44	13 715	TDF + 3TC + EFV	2013
4	412	Male	40	15 931	AZT + 3TC + EFV	2010
4	372	Male	31	20 221	ABC + 3TC + EFV	2012
4	873	Male	47	22 300	AZT + 3TC + EFV	2007
4	434	Male	34	88 000	TDF + 3TC + FPV/r	2011
4	448	Male	27	154 504	TDF + 3TC + ATV/r	2012

3TC, lamivudine; ABC, abacavir; ART, antiretroviral therapy; ATV, atazanavir; AZT, zidovudine; EFV, efavirenz; FPV, fosamprenavir; FTC, emtricitabine; NVP, nevirapine; /r, boosted ritonavir; RAL, raltegravir; TDF, tenofovir.
[a] CD4$^+$ T-cells counts are expressed as number of cells/mL of whole blood.
[b] Viral load is expressed as copies/mL of plasma.
[c] Treatments were initiated according to Brazilian national guidelines at the time of treatment initiation.

starting DNA concentration ($\leq$100 ng/μL and >100 ng/μL, respectively), and DNase/RNase-free water to a total volume of 20 μL. Calculation of the optimum dilution of cellular DNA in the final PCR mix is detailed in Supplementary Fig. S2. Integrated proviral DNA was measured by the published methods of Tan et al. [23] and Vandergeeten et al. [24]. Both techniques are nested PCRs with a first round of amplification of HIV-1 LTR-Alu or Alu-Alu DNA fragments. The LTR-specific primer further includes a lambda-specific linker sequence to increase the specificity of the second reaction, which is a real-time PCR employing a fluorescent HIV-1-specific probe. The primers, probes and amplification conditions adopted were those described in the original publications. The technique of Tan et al. [23] was adapted to human PBMCs by starting with an initial genomic DNA concentration of 100 ng/μL and transferring a quantity of 9 μL of the first amplification product to the second amplification mix (final volume 20 μL). These starting quantities produced an optimal yield of amplification according to preliminary analyses similar to those described in Supplementary Fig. S2. Based on sample availability, analyses were conducted in duplicate for the method of Tan et al. [23] and in triplicate for that of Vandergeeten et al. [24]. Fluorescence curves were visualised using CFX Maestro software (Bio-Rad, Hercules, CA, USA), which automatically computes Ct values. Ct values derived from damping curves were discarded and anomalous Ct values of <10 were subjected to electrophoretic analyses and were compared with positive and negative controls derived from in vitro HIV-1-infected and mock-infected cells. The average Ct values of housekeeping genes (human β-globin for [23] and CD3 for [24]) were subtracted from the HIV-1 Ct values to obtain ΔCt values. The relative impact of treatments on proviral DNA was calculated as the $-\Delta\Delta$Ct (baseline ΔCt – ΔCt at 5 months of treatment), which provides the $\log_2$ fold change.

2.4. Nef sequence amplification

The *nef* gene including small stretches of the neighbouring 5′ and 3′ sequences was amplified by PCR from genomic DNA according to previously published techniques [25–30] and as detailed in the Supplementary methods.

2.5. Flow cytometry

For flow cytometry experiments, 5×10^5 PBMCs were first stained with the viability dye AmCyan LIVE/DEAD™ Fixable Aqua Dead Cell Stain Kit (Thermo Fisher Scientific) and were then stained for phenotypic markers of lymphocyte identity using allophycocyanin-Cy7 (APC-Cy7) anti-CD3 (BD Biosciences, Franklin Lakes, NJ, USA), APC anti-CD4 (e-bioscience, San Diego, CA, USA), fluorescein isothiocyanate (FITC) anti-CD25 (BD Biosciences), FITC anti-CD38 (BD Biosciences) and peridinin-chlorophyll-protein complex (PerCP) anti-CD69 (e-bioscience) [31]. For intracellular cytokine analysis, after staining for viability and surface markers, cells were fixed and made permeable using an Intracellular Fixation & Permeabilisation Buffer Set (eBioscience) according to the manufacturer's instructions and phycoerythrin (PE) anti-IL2 (R&D Biosystems, Minneapolis, MN, USA) antibodies. Flow cytometry analyses were carried out in an LSRFortessa™ Analyzer (BD Biosciences). The experiments were analysed using FlowJo v.9.8 software (Tree Star, Inc., Ashland, OR, USA).

2.6. Bioinformatics analyses

Sequences were saved in FASTA format and were analysed using the online phylogeny.fr software (https://www.phylogeny.fr/) [32], and the workflow for the analyses was selected using the 'à la carte' option of the website. T-coffee was selected for sequence alignment. Alignments were then adjusted using gBlocks. Given the low sequence variation within each patient, we allowed (i) smaller final blocks, (ii) gap positions within the final blocks and (iii) less strict flanking positions compared with the default settings. PhyML was used to prepare the phylogenetic trees. A robust post-hoc analysis was then applied to validate the results (bootstrapping procedure with 100 bootstraps). Trees were then rendered as phylograms, collapsing the tree branches having branch support values <50%. To ensure reproducibility, phylogenetic tree preparation was repeated using the parsimony method 'Tree Analysis Using New Technology' (TNT) and post-hoc resampling using both the Jackknife and the symmetric resampling methods.

2.7. Measurement of HIV-1 replication and integration upon auranofin treatment of in vitro-infected CD4$^+$ T-cells

The impact of auranofin on integrated DNA in vitro was estimated by infecting activated CD4$^+$ T-cells with either wild-type HIV-1 or the dual-colour fluorescent orange–green HIV-1 (OGH) reporter [33] (details in Supplementary methods).

2.8. Computational simulations

Computational simulations of latently HIV-1-infected cell dynamics were based on the system of differential equations developed by Rong and Perelson [34], applying the baseline parameters as shown by the same authors. Numerical simulations were performed with the ordinary differential equations' solver of the MATLAB® software. The proliferation-upon-activation rate (*proliferation rate*; normal rate, 1.4 day^{-1}) was decreased proportionally to the result obtained in the experiment described in the previous paragraph.

2.9. Statistical analyses

Data analyses were conducted using GraphPad Prism v.7.02 (GraphPad Software Inc., San Diego, CA, USA). Differences between proportions were calculated using the χ^2 test or Fisher's exact test. Differences in proviral DNA for both techniques adopted were analysed by two-way analysis of variance (ANOVA) followed by post-hoc false discovery rate (FDR) multiple comparison analysis [level of significance for the adjusted *P*-value (q) = 0.05]. Where there was no previous indication of an effect, double-tailed tests were adopted. Correlation between variables was obtained by linear regression or by non-linear regression if the former was not applicable such as in the case of bell-shaped curves. For in vitro results, data were expressed as $\log_2$ fold change expression in CD4$^+$ T-cells treated with auranofin compared with untreated cells. Values of fold changes relative to experiments with wild-type HIV-1 and dual-colour OGH virus [33] were pooled and were compared with the null hypothesis (i.e. $\log_2$ fold change = 0) by one-sample *t*-test. Differences in activation markers were analysed by ANOVA following LOGIT transformation to restore normality.

3. Results

3.1. Safety

Experimental treatments were conducted in subjects under ART who had displayed stably undetectable viral loads with a first-line therapy according to the Brazilian national guidelines. Patients were enrolled and randomised as described in the flow chart in Supplementary Fig. S1. A 5-month timeframe for the auranofin treatment was chosen because it coincides with plateauing plasma and tissue levels of the drug [21]. Within the timeframe considered in this report, all of the patients recruited adhered to the protocol assigned and no dropouts from the study were observed. Auranofin treatment was well tolerated. In general, no major side effects were reported, and the overall health condition of the enrolled subjects remained satisfactory (Table 2). No severe (grade 3 or 4) events were observed in any of the treatment groups analysed. Addition of auranofin was not associated with an increased occurrence of clinical or laboratory events compared with the ART-only regimens considered [odds ratio (OR) = 1.00, 95% confidence interval (CI) 0.58–1.71 for clinical events; and OR = 1.17, 95% CI 0.51–2.66 for laboratory events]. None of the treatments affected viral loads, which remained permanently below the limit of detection of the assay (40 copies of viral RNA/mL of plasma; Supplementary Fig. S3). In line with the mechanism of action of the drug, the auranofin-treated group showed a transient decrease in CD4$^+$ T-cell counts at Weeks 8 and 12 (Fig. 1).

3.2. Impact of auranofin on total HIV-1 DNA

As an estimate of the viral reservoir, total viral DNA was measured using a previously published qPCR technique [22]. Auranofin decreased viral DNA in PBMCs (Fig. 2). Due to the small number of patients enrolled per arm, it was not possible to estimate the impact of the different ART regimens on viral DNA. To minimise any bias residing in reportedly imprecise viral nucleic acid quantification such as outlier value effects (e.g. Fig. 2D), a χ^2 analysis was performed estimating only the relative impact of auranofin on HIV-1 DNA. When auranofin-treated patients were compared with ART-only-containing regimens, a significantly higher number of patients experienced a decrease in viral DNA (P = 0.0365; OR = 9.75, 95% CI 1.10–72.39).

Table 2
List of adverse events recorded in each of the treatment groups.

Adverse event	No. (%) of patients [grade]			Total no.
	Group 1	Group 2	Group 4	
Any clinical event	5 (100%) [1]	3 (60%) [1,2]	4 (80%) [1,2]	12
Grade 3–4 event	0	0	0	0
Diarrhoea		1 (20%) [1]	3 (60%) [1,1,2]	4
Sore throat	1 (20%) [1]			1
Dizziness		1 (20%) [1]		1
Asthma			1 (20%) [1]	1
Sinus infection	1 (20%) [1]			1
Dyspepsia	1 (20%) [1]			1
Nephritic colic	1 (20%) [1]			1
Pruritus	1 (20%) [1]			1
Fracture of 5th finger		1 (20%) [2]		1
Any laboratory event	2	5	3	10
g-GT	1 [1]	2 [1]		3
LDL cholesterol	1 [1]			1
ALT		2 [1]	1 [1]	3
Creatinine		1 [1]	1 [2]	2
Triglycerides			1 [1]	1

g-GT, gamma-glutamyl transferase; LDL, low-density lipoprotein; ALT, alanine aminotransferase.

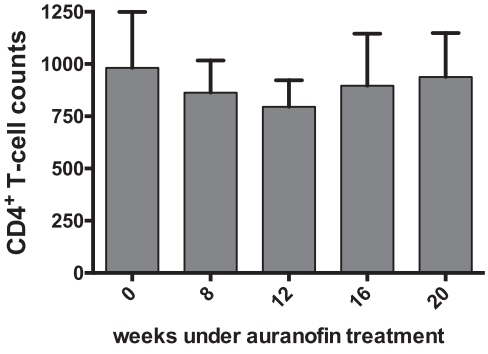

Fig. 1. Dynamics of CD4$^+$ T-cell counts in patients treated with intensified antiretroviral therapy + auranofin. CD4$^+$ T-cell numbers (cells/μL) were assessed by flow cytometry starting from the first administration of auranofin (Week 0).

3.3. Impact of auranofin on integrated HIV-1 DNA

As gold salts have been shown to exert an antiretroviral effect by interacting with the nucleocapsid protein of HIV-1 [35], the viral DNA changes in group 2 (intensified ART) and group 4 (intensified ART + auranofin) were further characterised by specific measurement of integrated viral DNA using two different Alu PCR techniques [23,24]. As a measure of precaution, the results were expressed in terms of relative amplification of integrated HIV-1. Fig. 3 shows the relative (within-subject) change of integrated DNA in the two groups ($-\Delta\Delta$Ct). The analyses showed a significant decrease of the integrated HIV-1 DNA over time only in the intensified ART + auranofin group according to both techniques (Fig. 3).

Along the lines of previous literature data [36], the analyses in Fig. 3 showed significant discrepancies between techniques. Therefore, we decided to further investigate this issue by conducting a correlation analysis of the results obtained. Although no

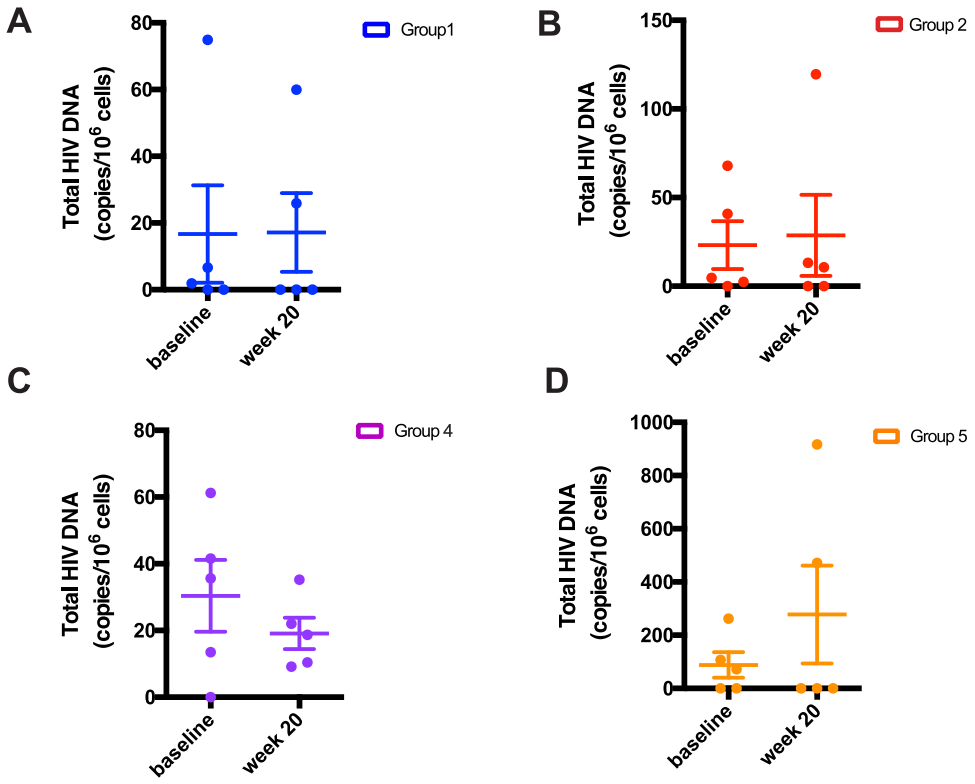

Fig. 2. Levels of total HIV-1 viral DNA in different treatment groups: (A) ART controls; (B) intensified ART; (C) intensified ART + auranofin; and (D) partially intensified ART (dolutegravir). Values at Weeks 0 and 20 after experimental treatment initiation. ART, antiretroviral therapy.

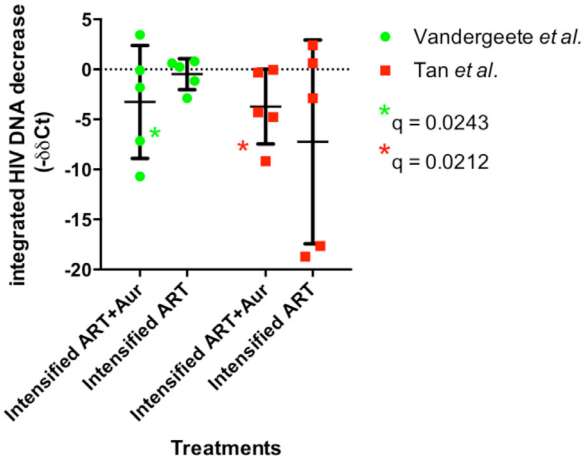

Fig. 3. Relative levels of integrated HIV-1 viral DNA in peripheral blood mononuclear cells (PBMCs) of patients treated with intensified antiretroviral therapy (ART) with or without auranofin (Aur). Levels of integrated viral DNA were assessed by Alu PCR according to the methods described in Tan et al. [23] and Vandergeeten et al. [24]. Data are shown as $\log_2$ fold change in viral DNA (the lower the $-\Delta\Delta$Ct value, the less viral DNA). Bars show the means ± standard error of the mean. q is the P-value corrected for multiple comparisons by controlling the false discovery rate (threshold for significance, $q = 0.05$).

significant correlation between techniques was at first detected (Pearson's correlation, $P = 0.7911$; Supplementary Fig. S4), a correlation trend became apparent if two outlier values ($-\Delta\Delta$Ct difference between techniques >15) were excluded (Pearson's correlation test, $P = 0.074$; Supplementary Fig. S4). By pooling the results of all techniques adopted (including total viral DNA measurement, indicated by some to be a less ambitious but more realistic marker of the viral reservoir [37]), the median size of the viral DNA pool during treatment with auranofin amounted to 11% of pre-treatment values (range, 7.5–30%).

3.4. Qualitative impact of auranofin on viral DNA composition

The composition of the viral DNA pools was then assessed to further analyse the impact of auranofin. Recent studies have suggested that a consistent proportion of HIV-1 DNA is maintained by a limited number of proliferating clones [38–40]. If auranofin indeed has an impact on HIV-1 DNA by inhibiting cell proliferation, the contribution of the original main clones to viral diversity should decrease or disappear and the composition of the viral DNA should change during auranofin treatment. To test this hypothesis, the *nef* gene and small stretches of the neighbouring 5′ and 3′ sequences (*env* and LTR) of the HIV-1 DNA obtained from PBMCs of three HIV-1-infected individuals subjected to treatment with intensified ART or intensified ART + auranofin were sequenced and the evolution of viral sequences over time was analysed (as detailed in Supplementary methods). The *nef* gene was chosen because of its relatively high within-host diversity and its ability to represent the diversity of viral DNA copies that are not truncated [41,42]. Results showed that the sequences from Month 5 of the intensified ART-only-treated individual 2-1 were strongly intermingled with closely related sequences prevalent at Month 1; a similar, albeit less pronounced, trend was observed in subject 2-3 (Fig. 4). This trend matches the observation that viral evolution and diversification do not occur over long-term suppressive ART as shown in several studies [43–49]. However, in patient 2-2, sequences from Month 1 and Month 5 were clearly phylogenetically distinct.

Such distinct and separate clustering between sequences isolated at Months 5 and 1 was observed in all three available sets of sequences from patients who had received intensified ART with auranofin (Fig. 4). The proportion of intensified ART + auranofin-treated individuals showing a distinct clustering of sequences (3/3)

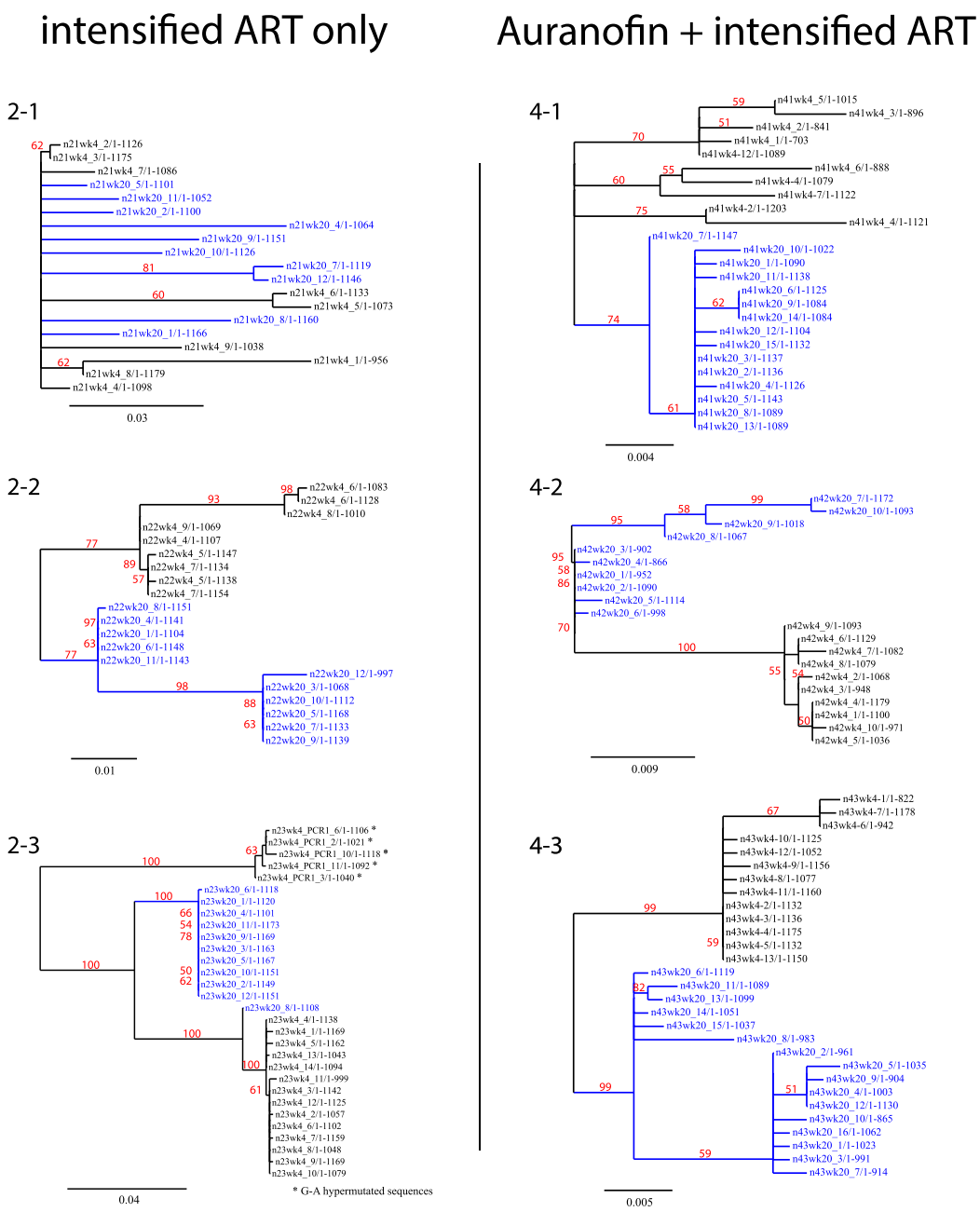

Fig. 4. Phylogenetic trees of HIV-1 *nef* sequences. Sequences were isolated from HIV-1-infected individuals at Month 1 (black) and Month 5 (blue) of treatment with intensified ART-only and intensified ART + auranofin. Bootstrap branch support values are displayed in red. ART, antiretroviral therapy.

was significantly different from that observed in the intensified ART-only group (difference between proportions, $P = 0.0416$). This trend suggests that the bulk of the original proviral sequences were decreased or depleted by the treatment and that auranofin might affect the composition of the circulating viral DNA.

3.5. In vitro antiproliferative effect of auranofin predicts in vivo reservoir reduction

The techniques adopted to analyse viral DNA in ART-treated individuals do not allow highlighting the replication-competent viral reservoir because 90% of the integrated viral DNA is likely to be defective [50]. Thus, to provide an estimate of the impact of the antiproliferative effect of auranofin on the viral reservoir, in vitro data obtained from primary CD4$^+$ T-cells was combined with mathematical modelling. Specifically, we used a widely adopted system of differential equations [34], which takes into account a number of variables, including proliferation upon activation, and adjusted this parameter based on the results obtained in vitro with a concentration of auranofin corresponding to its steady-state levels (Supplementary methods; Supplementary Fig. S5).

In the auranofin-treated condition, the proliferation rate was lowered from 1.4 day^{-1} (normal rate) to 0.56 day^{-1}, i.e. in proportion to the results of the in vitro experiments. All other baseline parameters were kept the same as those originally described by Rong and Perelson [34]. The results showed that upon auranofin treatment, the viral reservoir is expected to decay to 37% of the original level (Fig. 5A), a decrease slightly less pronounced than the range (7.5–30%) calculated from the ex vivo viral DNA data (Figs. 2 and 3).

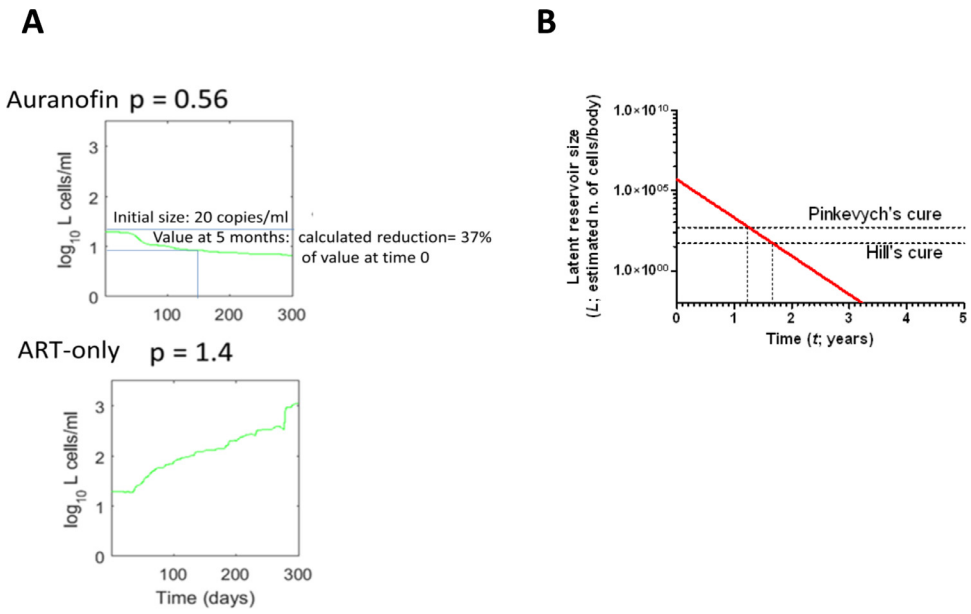

Fig. 5. Mathematical modelling of the decay of the HIV-1 reservoir over time following antiproliferative interventions. (A) Numerical simulations of programmed expansion and contraction of the viral reservoir. A simulation of the viral reservoir (L cells) dynamics in a human model is provided. The simulation is based on the five differential equations model in [34]. For starting data, see the same reference. Different proliferation rates (p) are shown (day^{-1}), corresponding to the auranofin-induced decrease (top panel) and to a scenario of a patient treated with antiretroviral therapy (ART) only (bottom panel). The activation function adopted to simulate lymphocyte encounter with antigens is illustrated in [34]. (B) Long-term projection of the impact of auranofin on the viral reservoir. An estimate of the long-term impact of auranofin on the viral reservoir is provided here with the 'composite interest' formula, assuming a constant decay of the HIV-1 reservoir: $L = 5 \times 10^5 \bullet (1–DR)^t$, where L is the reservoir size, DR is its decrease rate in the unit of time, t is the time from therapy initiation, and 5×10^5 (cells) is the initial value, as reported in [34]. Previously published cure thresholds [57,58] are shown by the dotted lines.

3.6. Effect of auranofin on activation/proliferation markers of CD4$^+$ T-cells

To investigate whether treatment with auranofin might have had an impact on activation, and consequently proliferation, of CD4$^+$ T-cells in HIV-1-infected individuals under ART, the levels of CD4$^+$ T-lymphocytes expressing well-validated immune activation/proliferation markers in HIV-1 infection were measured, i.e. CD38, HLA-DR, CD69 [51,52] and intracellular IL-2, a cytokine known to induce T-cell activation/proliferation [53].

It was found that both groups treated with intensified ART (group 2) and intensified ART + auranofin (group 4) displayed a decreased percentage of CD4$^+$CD38$^+$ (group 2, $P = 0.046$; group 4, $P = 0.0082$; Supplementary Fig. S6) and CD4$^+$HLA-DR$^+$ T-cells (group 2, $P = 0.003$; group 4, 0.033; Supplementary Fig. S6). This decrease was likely to be due to the inhibition of lymphocyte activation exerted by maraviroc at a different level [54]. Instead, only treatment with intensified ART/auranofin significantly decreased expression of CD69, a surface lymphocyte molecule inducing T-cell proliferation through IL-2 synthesis (group 2, $P = 0.982$; group 4, $P < 0.0001$; Supplementary Fig. S6). This phenomenon was associated with decreased intracellular expression of IL-2, although, due to the low number of subjects enrolled, this decrease was not statistically significant (Supplementary Fig. S6).

4. Discussion

The results of this study suggest that auranofin might have an impact on viral DNA dynamics through an antiproliferative effect, as inferred from all tests conducted. To estimate the potential effect of auranofin on the HIV-1 reservoir, viral DNA (both total and integrated) was used as a surrogate marker. For these analyses, a conservative approach was followed by taking into account only relative values of integrated HIV-1 DNA. Moreover, different techniques, including phylogenetic analyses, were employed to confirm the results obtained.

The sequence analyses indicated that auranofin may enhance diversification of viral DNA over time. Based on previous reports [15,16], we envision that such an effect mainly reflects restriction of the clonal expansion of HIV-1-infected cells. In this regard, ART intensification through maraviroc, a drug previously shown to have a possible impact on viral DNA [54,55], might have influenced the diversification of HIV-1 DNA sequences over time.

The in vitro and ex vivo data, coupled with mathematical modelling, showed that the antiproliferative effect of auranofin may be a major driver of the HIV-1 DNA dynamics detected in vivo. That the replication-competent viral reservoir might be similarly restricted by the antiproliferative effect of auranofin is suggested by a comparison of the current in vivo data with results from a mathematical model. This model has previously been able to simulate the viral load and viral reservoir dynamics occurring in HIV-1-infected individuals and SIV-infected macaques treated with ART [34,54]. However, the mathematical model employed may not take into account a number of events occurring in vivo, e.g. the possible anti-reservoir effects of CCR5 blockade [54,55]. Moreover, additional effects of auranofin, such as its pro-apoptotic and pro-differentiating action, might have contributed to the result obtained [17].

Whilst this study reports on the first use of auranofin in ART-treated HIV-1-infected individuals, it presents some limitations, such as the small number of patients enrolled and HIV-1 DNA sequences obtained. Furthermore, HIV-1 integration sites were not evaluated, precluding more definite conclusions regarding HIV-1-infected cell clonal expansion in the current study. For these reasons, it is difficult to discern between the impact of auranofin and ART intensification. Moreover, we confirm that discordance between methods for viral reservoir detection is a major problem affecting research on an HIV-1 cure at present. As previously shown by Eriksson et al. [36], there is a high level of divergence between techniques, with absolute integrated HIV-1 DNA values sometimes being higher than the total DNA values. Finally, the choice of conducting this first trial only in male subjects was driven by the need

to exclude complications from potential teratogenic effects of auranofin and, more recently, dolutegravir [20,56].

The study subjects of this trial may still be representative of the HIV-1-infected population in the Americas, where the epidemic is still most prevalent in men who have sex with men [57]. The interim analysis of this phase II trial shows that auranofin administration in combination with intensified ART is well tolerated in this population. A transient decline in $CD4^+$ T-cell counts in the auranofin-treated group was the only side effect clearly attributable to the drug and was consistent with its antilymphoproliferative effect [15]. In line with the good safety profile observed in this trial, future studies may diversify enrolment to ensure the reproducibility of the results in a broader population, including women and children.

The significance of these findings for the HIV-1 cure field is supported by a further mathematical simulation of the long-term impact of antiproliferative agents on the viral reservoir size. Our forecast based on analysis of data from this clinical trial using the compound interest approach (Fig. 5B) shows that, in a timeframe of <2 years, viral DNA would decrease to levels below previously calculated HIV-1 cure thresholds [58,59], further decreasing the number of cells infected with HIV-1 competent strains in a scenario where defective HIV-1 is already prevalent owing to long-term effective ART [60]. This projection is in line with a recent calculation of the HIV-1 curing potential of disease-modifying antiproliferative agents, which is based on a different method and on data from another clinical trial (using mycophenolate) [61]. Unfortunately, long-term administration of auranofin is discouraged owing to loss of activity and possible toxicity, and for this reason the current clinical trial planned auranofin administration for only 6 months. Therefore, addition of other agents such as the glutathione inhibitor buthionine sulfoximine (BSO), which is able to increase the antiproliferative effect of auranofin [62], might be necessary to accelerate the decay of the viral reservoir during the timeframe in which auranofin treatment is safest. Combining BSO with auranofin was previously shown to induce a functional cure of the infection in SIV-infected macaques [15,62], and a clinical trial is being planned to test whether this effect could be reproducible in humans. In this regard, our need to estimate the effects of auranofin in HIV-1-infected individuals under ART before adding a second oxidative stress-enhancing drug was the main reason behind the planning of this interim analysis. Alternatively, other agents that possess auranofin-like properties but are tolerated for longer could be administered for a prolonged attack on the viral reservoir. Finally, structured treatment interruptions will be necessary in future clinical trials to assess the anti-reservoir impact of auranofin-containing regimens.

Acknowledgments

The authors are thankful to Dr Shailendra Rathore (UCL, London, UK) for computational assistance in mathematical simulations; to Dora@hivforum (http://hivforum.info/forum/index.php) for providing an expert activist's feedback on the manuscript; and to Eric Verdin (Buck Institute, Novato, CA, USA) for providing the OGH construct. The authors are also thankful to Torino Pharma (San Diego, CA, USA) for providing auranofin and to ViiV Healthcare (Brentford, UK) for providing dolutegravir and maraviroc. Special thanks to the volunteers involved in the trial.

Declarations

Funding: This study was supported by grants from Fundacão de Amparo à Pesquisa do Estado de São Paulo (FAPESP, São Paulo, Brazil) [grant 13/11323-5 to RSD], the Brazilian National Research Council (CNPq, Brazil) [grant CNPq/cura 454700/14-8 to RSD], and the Deutsches Zentrum für Infektionsforschung (DZIF, Braunschweig, Germany) [04.704 to ML and 04.810 to ML and OF]. ViiV Healthcare (Brentford, UK) and Torino Pharma (San Diego, CA, USA) donated some of the study drugs. AS is supported by the Italian Ministry of Financial Affairs (Rome, Italy); ILS is supported by the DZIF and the Alexander von Humboldt-Stiftung (Bonn, Germany). The funders had no role in study design, data collection and analysis, the decision to present the data, or preparation of the manuscript.

Competing interest: AS, ML and ILS are inventors of patents covering the use of auranofin in HIV-1 infection. All other authors declare no competing interests.

Ethical approval: The protocol was approved by the Human Subjects Review Committee of the Federal University of Sao Paulo (Sao Paulo, Brazil) [approval no. 10757312.0.0000.5505].

Supplementary materials

Supplementary material associated with this article can be found, in the online version, at doi:10.1016/j.ijantimicag.2019.08.001.

References

[1] AbdelKhalek A, Abutaleb NS, Mohammad H, Seleem MN. Antibacterial and antivirulence activities of auranofin against *Clostridium difficile*. Int J Antimicrob Agents 2019;53:54–62.
[2] Thangamani S, Mohammad H, Abushahba MFN, Sobreira TJP, Seleem MN. Repurposing auranofin for the treatment of cutaneous staphylococcal infections. Int J Antimicrob Agents 2016;47:195–201.
[3] Hopper M, Yun J-F, Zhou B, Le C, Kehoe K, Le R, et al. Auranofin inactivates *Trichomonas vaginalis* thioredoxin reductase and is effective against trichomonads in vitro and in vivo. Int J Antimicrob Agents 2016;48:690–4.
[4] Norton S. A brief history of potable gold. Mol Interv 2008;8:120–3.
[5] Thangamani S, Maland M, Mohammad H, Pascuzzi PE, Avramova L, Koehler CM, et al. Repurposing approach identifies auranofin with broad spectrum antifungal activity that targets Mia40-Erv1 pathway. Front Cell Infect Microbiol 2017;7:4.
[6] Langsjoen RM, Auguste AJ, Rossi SL, Roundy CM, Penate HN, Kastis M, et al. Host oxidative folding pathways offer novel anti-chikungunya virus drug targets with broad spectrum potential. Antiviral Res 2017;143:246–51.
[7] Chomont N, El-Far M, Ancuta P, Trautmann L, Procopio FA, Yassine-Diab B, et al. HIV reservoir size and persistence are driven by T cell survival and homeostatic proliferation. Nat Med 2009;15:893–900.
[8] Siliciano JD, Siliciano RF. Recent developments in the effort to cure HIV infection: going beyond N = 1. J Clin Invest 2016;126:409–14.
[9] Massanella M, Fromentin R, Chomont N. Residual inflammation and viral reservoirs: alliance against an HIV cure. Curr Opin HIV AIDS 2016;11:234–41.
[10] Maldarelli F. The role of HIV integration in viral persistence: no more whistling past the proviral graveyard. J Clin Invest 2016;126:438–47.
[11] Hütter G. Stem cell transplantation in strategies for curing HIV/AIDS. AIDS Res Ther 2016;13:31.
[12] Gupta RK, Abdul-Jawad S, McCoy LE, Mok HP, Peppa D, Salgado M, et al. HIV-1 remission following CCR5Δ32/Δ32 haematopoietic stem-cell transplantation. Nature 2019;568:244–8. doi:10.1038/s41586-019-1027-4.
[13] Hütter G, Nowak D, Mossner M, Ganepola S, Müssig A, Allers K, et al. Long-term control of HIV by CCR5 Delta32/Delta32 stem-cell transplantation. N Engl J Med 2009;360:692–8.
[14] Lewis MG, DaFonseca S, Chomont N, Palamara AT, Tardugno M, Mai A, et al. Gold drug auranofin restricts the viral reservoir in the monkey AIDS model and induces containment of viral load following ART suspension. AIDS 2011;25:1347–56.
[15] Vint IA, Chain BM, Foreman JC. The interaction of auranofin and buthionine sulfoximine blocks activation of human peripheral T lymphocytes. Cell Immunol 1993;152:152–61.
[16] Shytaj IL, Nickel G, Arts E, Farrell N, Biffoni M, Pal R, et al. Two-year follow-up of macaques developing intermittent control of the human immunodeficiency virus homolog simian immunodeficiency virus SIVmac251 in the chronic phase of infection. J Virol 2015;89:7521–35.
[17] Chirullo B, Sgarbanti R, Limongi D, Shytaj IL, Alvarez D, Das B, et al. A candidate anti-HIV reservoir compound, auranofin, exerts a selective 'anti-memory' effect by exploiting the baseline oxidative status of lymphocytes. Cell Death Dis 2013;4:e944.

[18] Psomas CK, Fidler S, Macartney M, Jeffreys R, Reilly L, Collins S, et al. Highlights from the 22nd International AIDS Conference (AIDS 2018), 22–27 July 2018, Amsterdam, the Netherlands. J Virus Erad 2018;4:238–47.
[19] Badley AD, Sainski A, Wightman F, Lewin SR. Altering cell death pathways as an approach to cure HIV infection. Cell Death Dis 2013;4:e718.
[20] Gao X-Y, Li K, Jiang L-L, He M-F, Pu C-H, Kang D, et al. Developmental toxicity of auranofin in zebrafish embryos. J Appl Toxicol 2017;37:602–10.
[21] Lewis D, Capell HA, McNeil CJ, Iqbal MS, Brown DH, Smith WE. Gold levels produced by treatment with auranofin and sodium aurothiomalate. Ann Rheum Dis 1983;42:566–70.
[22] Buzón MJ, Massanella M, Llibre JM, Esteve A, Dahl V, Puertas MC, et al. HIV-1 replication and immune dynamics are affected by raltegravir intensification of HAART-suppressed subjects. Nat Med 2010;16:460–5.
[23] Tan W, Dong Z, Wilkinson TA, Barbas CF 3rd, Chow SA. Human immunodeficiency virus type 1 incorporated with fusion proteins consisting of integrase and the designed polydactyl zinc finger protein E2C can bias integration of viral DNA into a predetermined chromosomal region in human cells. J Virol 2006;80:1939–48.
[24] Vandergeeten C, Fromentin R, Merlini E, Lawani MB, DaFonseca S, Bakeman W, et al. Cross-clade ultrasensitive PCR-based assays to measure HIV persistence in large-cohort studies. J Virol 2014;88:12385–96.
[25] Galaski J, Ahmad F, Tibroni N, Pujol FM, Müller B, Schmidt RE, et al. Cell surface downregulation of NK cell ligands by patient-derived HIV-1 Vpu and Nef alleles. J Acquir Immune Defic Syndr 2016;72:1–10.
[26] Brodin J, Krishnamoorthy M, Athreya G, Fischer W, Hraber P, Gleasner C, et al. A multiple-alignment based primer design algorithm for genetically highly variable DNA targets. BMC Bioinformatics 2013;14:255.
[27] Yoon H, Leitner T. PrimerDesign-M: a multiple-alignment based multiple-primer design tool for walking across variable genomes. Bioinformatics 2015;31:1472–4.
[28] Villanova F, Barreiros M, Janini LM, Diaz RS, Leal É. Genetic diversity of HIV-1 gene *vif* among treatment-naive Brazilians. AIDS Res Hum Retroviruses 2017;33:952–9.
[29] Gräf T, Pinto AR. The increasing prevalence of HIV-1 subtype C in Southern Brazil and its dispersion through the continent. Virology 2013;435:170–8.
[30] Kumar M, Jain SK, Pasha ST, Chattopadhaya D, Lal S, Rai A. Genomic diversity in the regulatory *nef* gene sequences in Indian isolates of HIV type 1: emergence of a distinct subclade and predicted implications. AIDS Res Hum Retroviruses 2006;22:1206–19.
[31] Vatakis DN, Nixon CC, Bristol G, Zack JA. Differentially stimulated CD4$^+$ T cells display altered human immunodeficiency virus infection kinetics: implications for the efficacy of antiviral agents. J Virol 2009;83:3374–8.
[32] Dereeper A, Audic S, Claverie J-M, Blanc G. BLAST-EXPLORER helps you building datasets for phylogenetic analysis. BMC Evol Biol 2010;10:8.
[33] Vranckx LS, Demeulemeester J, Saleh S, Boll A, Vansant G, Schrijvers R, et al. LEDGIN-mediated inhibition of integrase-LEDGF/p75 interaction reduces reactivation of residual latent HIV. EBioMedicine 2016;8:248–64.
[34] Rong L, Perelson AS. Modeling latently infected cell activation: viral and latent reservoir persistence, and viral blips in HIV-infected patients on potent therapy. PLoS Comput Biol 2009;5:e1000533.
[35] Spell SR, Mangrum JB, Peterson EJ, Fabris D, Ptak R, Farrell NP. Au(iii) compounds as HIV nucleocapsid protein (NCp7)–nucleic acid antagonists. Chem Commun 2017;53:91–4.
[36] Eriksson S, Graf EH, Dahl V, Strain MC, Yukl SA, Lysenko ES, et al. Comparative analysis of measures of viral reservoirs in HIV-1 eradication studies. PLoS Pathog 2013;9:e1003174.
[37] Avettand-Fènoël V, Hocqueloux L, Ghosn J, Cheret A, Frange P, Melard A, et al. Total HIV-1 DNA, a marker of viral reservoir dynamics with clinical implications. Clin Microbiol Rev 2016;29:859–80.
[38] Maldarelli F, Wu X, Su L, Simonetti FR, Shao W, Hill S, et al. HIV latency. Specific HIV integration sites are linked to clonal expansion and persistence of infected cells. Science 2014;345:179–83.
[39] Wagner TA, McLaughlin S, Garg K, Cheung CYK, Larsen BB, Styrchak S, et al. HIV latency. Proliferation of cells with HIV integrated into cancer genes contributes to persistent infection. Science 2014;345:570–3.
[40] Simonetti FR, Sobolewski MD, Fyne E, Shao W, Spindler J, Hattori J, et al. Clonally expanded CD4$^+$ T cells can produce infectious HIV-1 in vivo. Proc Natl Acad Sci U S A 2016;113:1883–8.
[41] Pinzone MR, VanBelzen DJ, Weissman S, Bertuccio MP, Cannon L, Venanzi-Rullo E, et al. Longitudinal HIV sequencing reveals reservoir expression leading to decay which is obscured by clonal expansion. Nat Commun 2019;10:728.
[42] Jones BR, Kinloch NN, Horacsek J, Ganase B, Harris M, Harrigan PR, et al. Phylogenetic approach to recover integration dates of latent HIV sequences within-host. Proc Natl Acad Sci U S A 2018;115:E8958–67.
[43] van Zyl G, Bale MJ, Kearney MF. HIV evolution and diversity in ART-treated patients. Retrovirology 2018;15:14.
[44] Brodin J, Zanini F, Thebo L, Lanz C, Bratt G, Neher RA, et al. Establishment and stability of the latent HIV-1 DNA reservoir. Elife 2016;5 pii: e18889. doi:10.7554/eLife.18889.
[45] Evering TH, Mehandru S, Racz P, Tenner-Racz K, Poles MA, Figueroa A, et al. Absence of HIV-1 evolution in the gut-associated lymphoid tissue from patients on combination antiviral therapy initiated during primary infection. PLoS Pathog 2012;8:e1002506.
[46] Bailey JR, Sedaghat AR, Kieffer T, Brennan T, Lee PK, Wind-Rotolo M, et al. Residual human immunodeficiency virus type 1 viremia in some patients on antiretroviral therapy is dominated by a small number of invariant clones rarely found in circulating CD4$^+$ T cells. J Virol 2006;80:6441–57.
[47] Kearney MF, Spindler J, Shao W, Yu S, Anderson EM, O'Shea A, et al. Lack of detectable HIV-1 molecular evolution during suppressive antiretroviral therapy. PLoS Pathog 2014;10:e1004010.
[48] Josefsson L, von Stockenstrom S, Faria NR, Sinclair E, Bacchetti P, Killian M, et al. The HIV-1 reservoir in eight patients on long-term suppressive antiretroviral therapy is stable with few genetic changes over time. Proc Natl Acad Sci U S A 2013;110:E4987–96.
[49] Wagner TA, McKernan JL, Tobin NH, Tapia KA, Mullins JI, Frenkel LM. An increasing proportion of monotypic HIV-1 DNA sequences during antiretroviral treatment suggests proliferation of HIV-infected cells. J Virol 2013;87:1770–8.
[50] Bruner KM, Murray AJ, Pollack RA, Soliman MG, Laskey SB, Capoferri AA, et al. Defective proviruses rapidly accumulate during acute HIV-1 infection. Nat Med 2016;22:1043–9.
[51] Paiardini M, Müller-Trutwin M. HIV-associated chronic immune activation. Immunol Rev 2013;254:78–101. doi:10.1111/imr.12079.
[52] Sousa AE, Carneiro J, Meier-Schellersheim M, Grossman Z, Victorino RM. CD4 T cell depletion is linked directly to immune activation in the pathogenesis of HIV-1 and HIV-2 but only indirectly to the viral load. J Immunol 2002;169:3400–6.
[53] Bangs SC, McMichael AJ, Xu XN. Bystander T cell activation—implications for HIV infection and other diseases. Trends Immunol 2006;27:518–24.
[54] Shytaj IL, Norelli S, Chirullo B, Della Corte A, Collins M, Yalley-Ogunro J, et al. A highly intensified ART regimen induces long-term viral suppression and restriction of the viral reservoir in a simian AIDS model. PLoS Pathog 2012;8:e1002774.
[55] Gutiérrez C, Díaz L, Vallejo A, Hernández-Novoa B, Abad M, Madrid N, et al. Intensification of antiretroviral therapy with a CCR5 antagonist in patients with chronic HIV-1 infection: effect on T cells latently infected. PLoS One 2011;6:e27864. doi:10.1371/journal.pone.0027864.
[56] Foster C, Fidler S, Lyall E, Taylor G. Careful consideration when responding to new data: dolutegravir and pregnancy. J Virus Erad 2018;4:208.
[57] Beyrer C, Baral SD, van Griensven F, Goodreau SM, Chariyalertsak S, Wirtz AL, et al. Global epidemiology of HIV infection in men who have sex with men. Lancet 2012;380:367–77.
[58] Hill AL, Rosenbloom DIS, Fu F, Nowak MA, Siliciano RF. Predicting the outcomes of treatment to eradicate the latent reservoir for HIV-1. Proc Natl Acad Sci U S A 2014;111:13475–80.
[59] Pinkevych M, Cromer D, Tolstrup M, Grimm AJ, Cooper DA, Lewin SR, et al. HIV reactivation from latency after treatment interruption occurs on average every 5–8 days—implications for HIV remission. PLoS Pathog 2015;11:e1005000 Erratum in: PLoS Pathog 2016;12:e1005745. doi:10.1371/journal.ppat.1005745.
[60] Samer S, Namiyama G, Oshiro T, Arif MS, Cardoso da Silva W, Sucupira MCA, et al. Evidence of noncompetent HIV after ex vivo purging among ART-suppressed individuals. AIDS Res Hum Retroviruses 2017;33:993–4.
[61] Reeves DB, Duke ER, Hughes SM, Prlic M, Hladik F, Schiffer JT. Anti-proliferative therapy for HIV cure: a compound interest approach. Sci Rep 2017;7:4011.
[62] Benhar M, Shytaj IL, Stamler JS, Savarino A. Dual targeting of the thioredoxin and glutathione systems in cancer and HIV. J Clin Invest 2016;126:1630–9.